Open Access **Baghdad Science Journal** **P-ISSN: 2078-8665**
Published Online First: April, 2023 **2023, 20(6): 2241-2248** **E-ISSN: 2411-7986**

DOI: https://dx.doi.org/10.21123/bsj.2023.7678

Effect of Chromium (VI) on the Oxidation of Methylene Blue Dye by Fe3O4/ Chitosan Composite

Yaman K. Sadiq* ***Khulood A. Saleh***

Department of Chemistry, College of Science, University of Baghdad, Baghdad, Iraq
*Corresponding author: yaman.khaled1205m@sc.uobaghdad.edu.iq
E-mail address: khulood_abid@yahoo.com

Received 2/9/2022, Revised 9/12/2022, Accepted 11/12/2022, Published Online First 20/4/2023, Published 01/12/2023

Abstract:

Heavy metal ion removal from industrial wastewater treatment systems is still difficult because it contains organic contaminants. In this study, functional composite hydrogels with photo Fenton reaction activity were used to decompose organic contaminants. Fe_3O_4 Nanoparticle, chitosan (CS), and other materials make up the hydrogel. There are different factors that affected Photo-Fenton activity including (pH, H_2O_2 conc., temp., and exposure period). Atomic force microscopy was used to examine the morphology of the composite and its average diameter (AFM). After 60 minutes of exposure to UV radiation, CS/ Fe_3O_4 hydrogel composite had degraded methylene blue (M.B.) dye by 92 percent. In the meantime, following an 1hour of visible irradiation, COD (Chemical Oxygen Demand) dropped to 6.1 mg/l.

Keywords: Adsorption, CS/Fe_3O_4 composite, Degradation, M.B. dye., Photo- Fenton reaction.

Introduction:

The introduction of toxins into the natural environment is referred to as pollution. There are many types of pollution (air pollution noise pollution, water pollution, soil pollution thermal pollution radiation pollution). The majority of illnesses are caused by environmental pollutants. Water is the primary source of contamination and pollution, which has a level of medical influence on human health. Harmful chemicals, dyes, oils, and other substances damage water. All effluent containing hazardous substances is discharged into neighboring bodies of water. This pollutes the water and produces a variety of health issues for the flora and wildlife. Dyes are a major contributor to water pollution. The majority of dyes emitted by the pharmaceutical and textile industries are carcinogenic, poisonous, and teratogenic, posing substantial health risks to humans and cattle. The evolution of modern, hygienic, and environmentally friendly purification technology has been prompted by environmental degradation and industrialization. Advanced oxidation mechanisms are extremely effective at consuming various hazardous, organic pollutants and completely destroying new contaminants such as naturally occurring poisons, pesticides, dyes, and other harmful contaminants. Whereas One of the most essential strategies for breaking down pollutants and forming environmentally beneficial goods is to use advanced oxidation processes (AOPs)[1]. There are various types of AOP; non-photochemical AOP procedures including ozonation or the Fenton reaction to generate hydroxyl radicals in the absence of light. UV light, H_2O_2, O_3, and/or Fe^{2+} are used in photolysis AOPs to create reactive hydroxyl radicals but photochemical methods are utilized when traditional O_3 and H_2O_2 are unable to thoroughly oxidize organic contaminants. The most important process in oxidation is Phot-Fenton, where it works on the generation of free radicals and in the presence of UV light[2], hydrogen peroxide and iron ions [3]. The treatment of non-biodegradable wastewater in the field of AOPs has made extensive use of Fenton and (Photo-Fenton) process [4]. Principled (AOP's) are based on the generation of OH radicals in the solution. These OH radicals then will be responsible for the oxidation of organic compounds and act with non-selectivity. The photo reaction will cause the formation of OH radicals[5]. AOPs have benefits and drawbacks, but the benefits outweigh the drawbacks for the most part.

1- There is a rapid reaction time.

2- There is a modest footprint.
3- The potential for reduced toxicity and total mineralization in the case of treated organics [6].

Experimental Part

Determination of Maximum Absorption (λ max)

M.B. dye is usually used because it can have used to calculate the surface area of any catalyst[7], to know the rate of degradation through photo Fenton reaction and considering the dye as a pollutant instead of polluted water. The M.B. was prepared at a concentration of 7 ppm by dissolving the solid powder from it with distilled water. The calibration curve of the dye was found and taken as plank for the next study. An ultraviolet visible absorption spectrum was performed for methylene blue (M.B.). The absorption spectrum is shown as peaks between absorbance and wavelength. The wavelength of (M.B.) dye's absorbance value was 661 nm. as shown in Fig. 1, which was conducted in several studies to find out the concentration before and after the reaction.

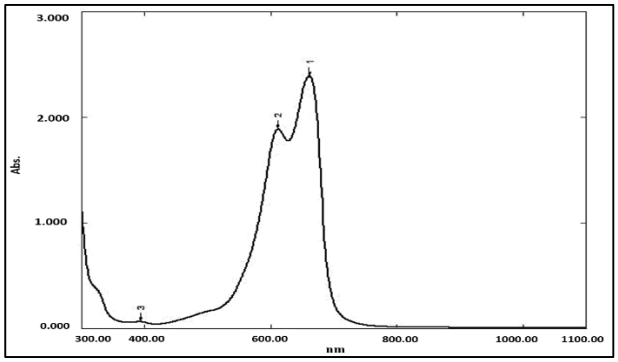

Figure 1. The absorption spectrum for M.B. dye by UV-Visible

The following Fig. 2 shows the calibration curve through which a linear equation is found through Beer-Lambert's law and the curve is represented between concentration and absorbance (A) using a spectrophotometer with a wavelength range 190-1100 nm.

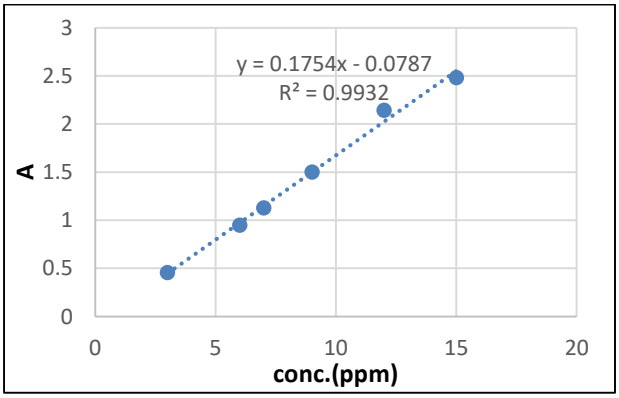

Figure 2. Calibration curve of M.B.

Synthesis of CS/Fe_3O_4 Nanocomposite

Good oxidizing nanocomposites was prepared in the Fenton reaction consisting of a mixture of a biopolymer, chitosan (purity:90% deacetylated) with iron(III) oxide, by suspension the chitosan in 1% acetic acid solution under continuous stirring for 10 minutes until it became well suspended. Then the iron oxide was added and the solution was dispersed in Ultrasonic device for 4 minutes to ensure that the particles are well distributed and that no agglomeration occurs. This is done at a temperature of 20°C, then the ammonium hydroxide solution was slowly added and put in the Ultrasonic device again, thus we got a homogeneous solution of magnetic composite. It was left to dry for 24 hours as shown in Fig. 3. After that we got a magnetic crystal powder and this powder was suspensed by distilled water and placed in the Fenton cell [8].

Figure 3. CS/Fe_3O_4 Composite

Preparation of Photocell

Stainless steel tube with a diameter of 4 cm and a length of 15 cm was equipped with a copper coil surrounding the outer cell surface and connected to a water bath to control of the reactor heat and lamp solution. First, concentrated HF acid is used to treat the inner cell surface, creating also, the cell or photo is rough on the inside and might pick up paint. To coat the photo cell, suspension solution of Chitosan/ Fe_3O_4 was decanted and allowed to make stable layer on the cell inner surface for 10 minute, on air drier 500° C was used to dry the coated layer[9]. To start studying the effect of Cr^{6+} on the photo-Fenton degradation of methylene blue dye, 20 ppm of Cr^{6+} (potassium dichromate) was used. Figure 4 shows the apparatus used in degradation process and the suspension composite which coated the cell.

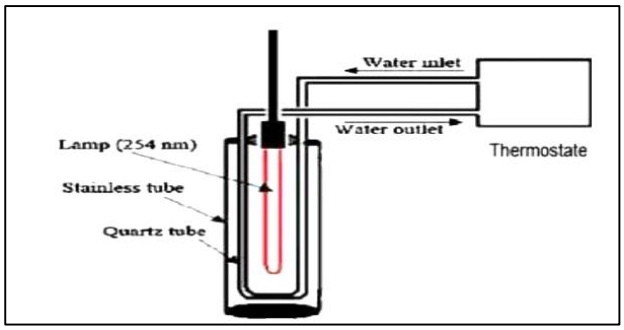

Figure 4. Setup for image degradation using the full system.

Results and Discussion

Characterization Study

In FTIR spectrum of CS as shown in Fig. 5, a broad band appears in CS spectrum at ν 3434.98,3417.63 cm^{-1} for (NH_2 stretching) groups and ν 3244.05 cm^{-1} of O-H stretching group. A peak at ν 2869.88 cm^{-1} can be characterized for C-H extending the aliphatic group's. C=O in amide groups ν 1637.45 cm^{-1}. (C-H, CH_2) aliphatic at ν 1469.66, 1415.65 cm^{-1} respectively. Other significant bands in CS can be found at ν 1340.43 cm^{-1} (C-N bending), ν 1149.50 cm^{-1} (anti-symmetrical of the C-O-C bridge), ν 1047.27 cm^{-1} (C-O bending of a saccharide structure) and ν 1020.27 cm^{-1} (O-H bending), C-C aliphatic appear at ν 925.77 cm^{-1}. Figure 6 indicates a shift in all peaks, and this is an evidence of the interaction that took place, as frequencies a broad band appears at ν 3452.34 cm^{-1} and 3434.98 cm^{-1} of NH_2 stretching groups. In ν 3292.26 cm^{-1} of O-H stretching group. A peak at ν 2875.67 cm^{-1} can be characterized for C-H extending the aliphatic group's. C=O in amide groups ν 1639.38 cm^{-1}. the appearance of a peak at ν 1413.72 cm^{-1} of CH_2 bending the aliphatic group. Other bands in CS can be found at ν 1367.44 cm^{-1} (C-N bending), ν 1153.35 cm^{-1} (anti-symmetrical of the C-O-C bridge), ν 1089.71 cm^{-1} (C-O bending of a saccharide structure) and ν 1047.27 cm^{-1} (O-H bending), C-C aliphatic appear at ν 943.13 cm^{-1} [10].

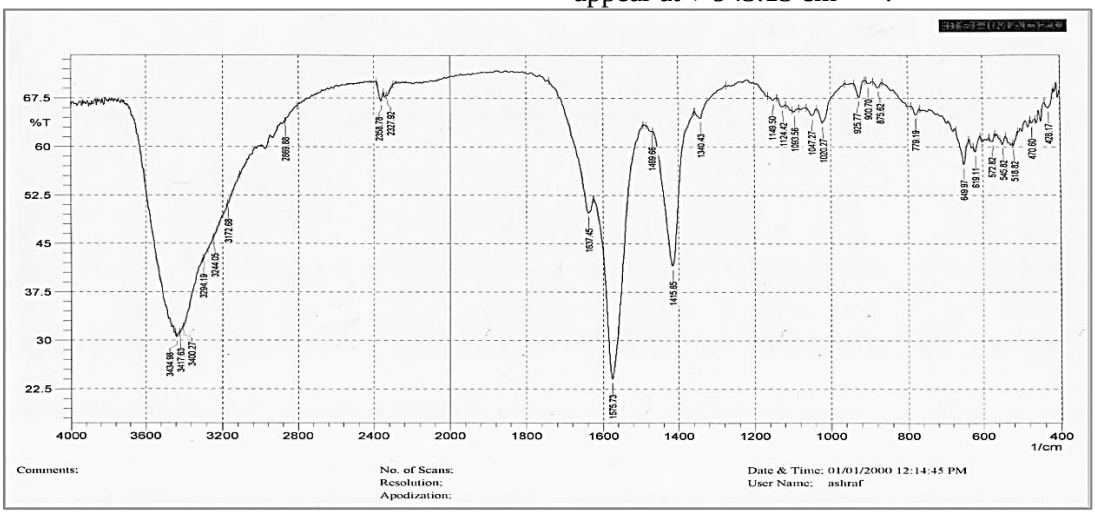

Figure 5. The FTIR spectrum of chitosan

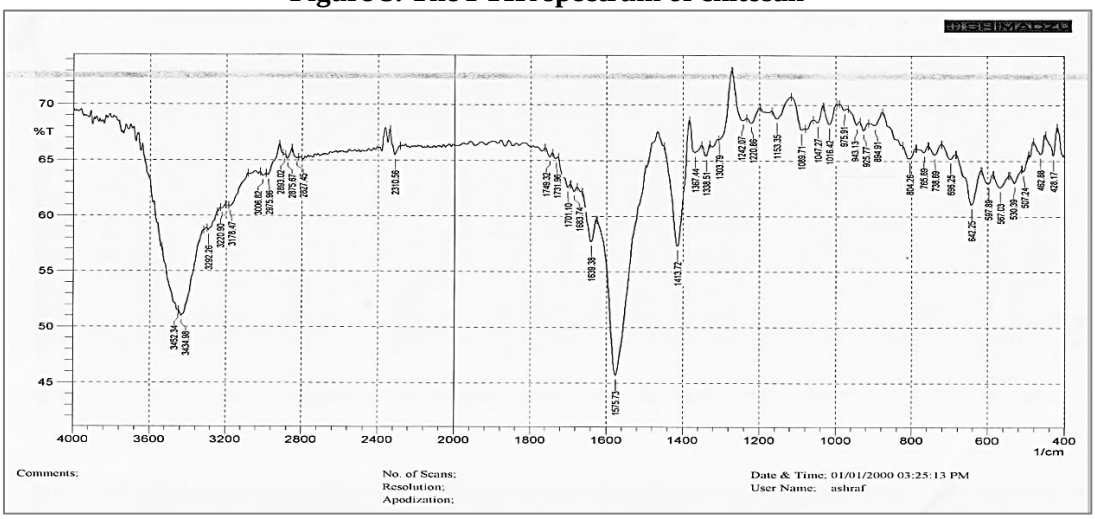

Figure 6. The FTIR spectrum of CS/ Fe_3O_4 composite

All of the diffraction peaks for chitosan in the XRD pattern, at 2θ = 12.958°, 21.771°, 28.102°, and at 2θ = 30.241°, 35.630°, 43.284°, 53.733°, 57.271°, and 62.925° for Fe_3O_4 may be quickly attributed to

the pure cubic magnetite structure, which is consistent with the results The peaks were distinct, and this suggests that the structural arrangement in the lengthy bands was at its best[11].

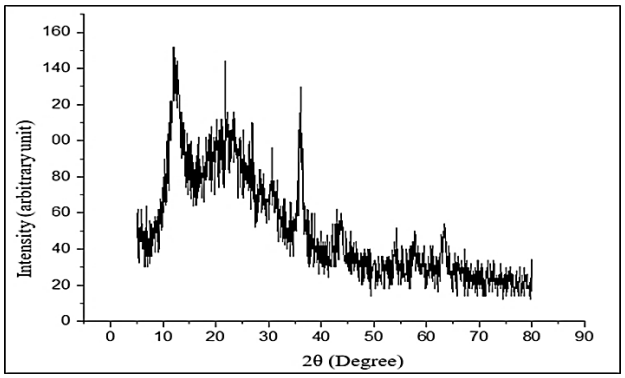

Figure 7. XRD pattern of CS/Fe_3O_4

tomic Force Microscope

The AFM study provides measurements of the average grain size and granularity cumulating distribution for the composite built of CS and Fe_3O_4. the most commonly used parameters are of average roughness (Sa) and square roughness (Sq). The data of CS/ Fe_3O_4 are (Roughness average= 8.455, average diameter= 13.65) nm, as shown in Fig. 8, average diameter to find out the diameter of the particle. When the surface area increases, number of reaction sites increases and the percentage degradation will be increased. While the roughness average has been used to compare the change of the morphology of the surface after treating with Fe_3O_4 [12].

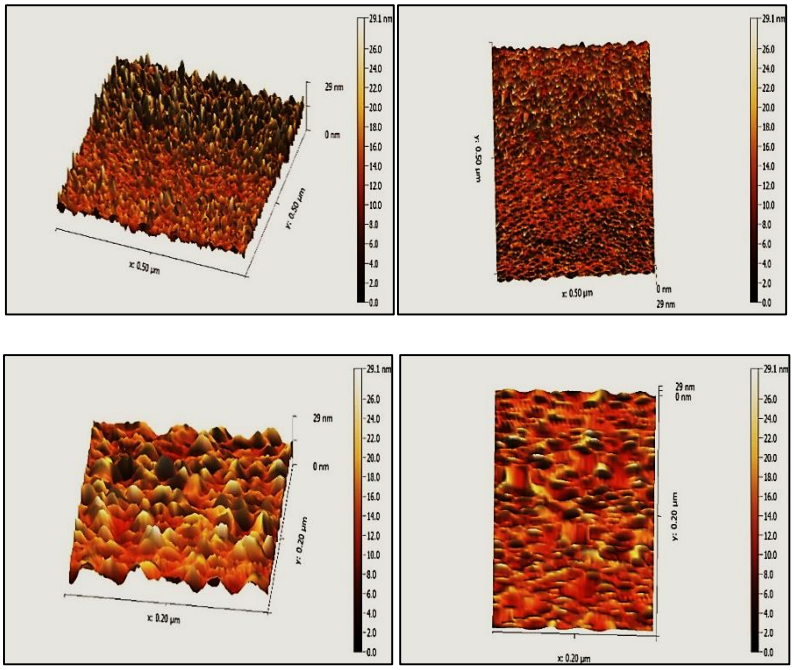

Figure 8. Atomic microscopy image of CS/ Fe_3O_4

Effect of Fenton Detector

At pH = 7, the effect of Fenton on the percent decomposition (% deg) of dye was studied using CS and CS/ Fe_3O_4 compound with Fenton reagent. The result shows that the presence of Fenton reagent with iron oxide is better than the primary coating and that it increases the degradation of M.B 7 ppm. After UV irradiation, the samples were quickly removed at different time intervals for spectrometry. A spectrophotometer was used to record the absorption spectra of the solutions produced. Using spectrophotometry, percentage degradation was calculated according to the literature [13],

$$\textbf{\% degradation} = \frac{\textit{initial conc.} - \textit{final con.}}{\textit{initial conc.}} * \mathbf{100}\% \quad 1$$

It was found that after one hour of 60 minutes, the rate of smashing had stabilized, as shown in Fig. 9.

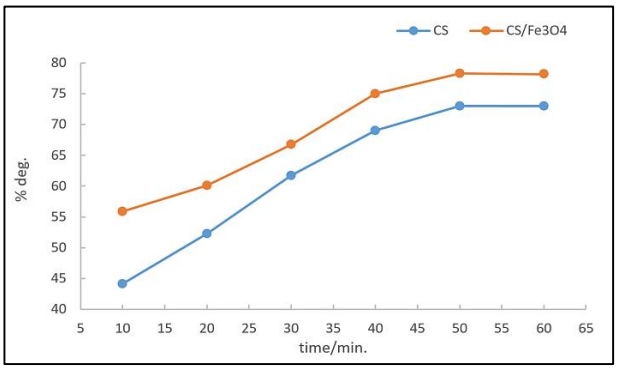

Figure 9. Variations of (% deg.) & time for M.B 7 ppm in presence of UV light at 298K, pH= 7 and by CS, CS/ Fe_3O_4 catalyst.

Effect of H_2O_2 Concentration

One of the operating factors that greatly affects the final mineralization extent is hydrogen peroxide concentration. When a specific ideal Fenton reagent ratio reaches, degradation efficiency also increases with additional increases in (H_2O_2 conc.). The effect of (H_2O_2 conc.) on the M.B degradation was studied at temperature 298 K, pH= 7 after 60 min in the presence of catalyst CS, CS/ Fe_3O_4 composite, and the % deg. increase with (H_2O_2 conc.) increased [14] as shown in Fig. 10.

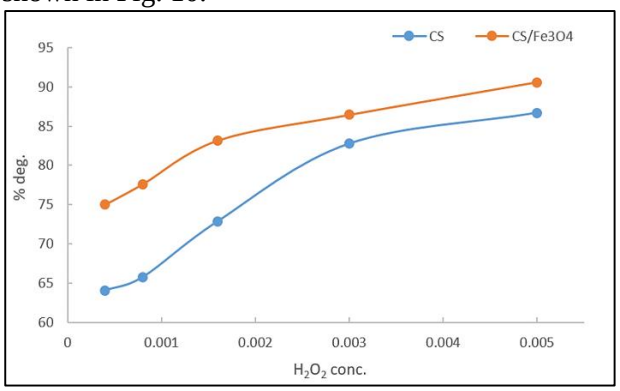

Figure 10. Effect of varying (H_2O_2 conc.) for 7 ppm M.B. after 60 min, at 298K, pH=7 on CS, CS/ Fe_3O_4 compound catalyst.

Effect of pH on Degradation Process

pH had an impact on the degradation of 7 ppm M.B after 60 minutes in the presence of CS Biomass and H_2O_2 $5*10^{-3}$M. The photolysis procedure was also carried out at altered pH settings using HCl 0.5M and NaOH 0.5M, while composites maintained constant levels of dye solutions. While when using the CS/Fe_3O_4 compound, the study of the effect of pH failed because deposition superimposed with the pollutant.

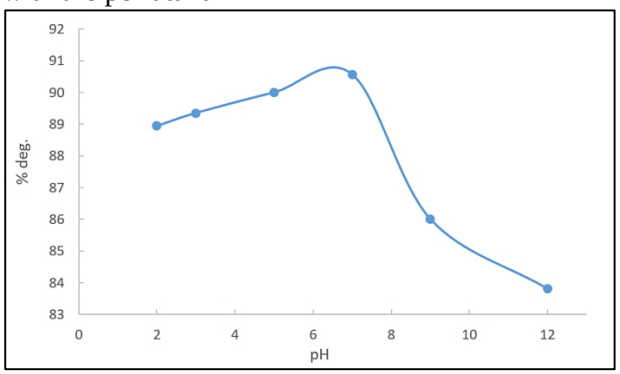

Figure 11. Percentage degradation Variation of 7 ppm M.B (% deg.) with different pH by CS catalyst and $5*10^{-3}$ M H_2O_2.

Effect of Cr^{6+} Ion Concentration

Chromium ion concentration had an effect on the % deg. at 7 ppm of MB after 60 minutes in the presence of CS and CS/ Fe_3O_4, hydrogen peroxide 5 * 10^{-3} M. The photolysis procedure was carried out using pH 7 and a temperature of 298 K, while the compounds maintained stable levels of the dye solutions. Where the chromium solution was placed with the pollutant which is the dye. During the use of the compound CS/ Fe_3O_4, the rate of deterioration was higher than that of chitosan. It was found that the optimum concentration of chromium used in this process was 20 ppm, Fig. 12 indicates that.

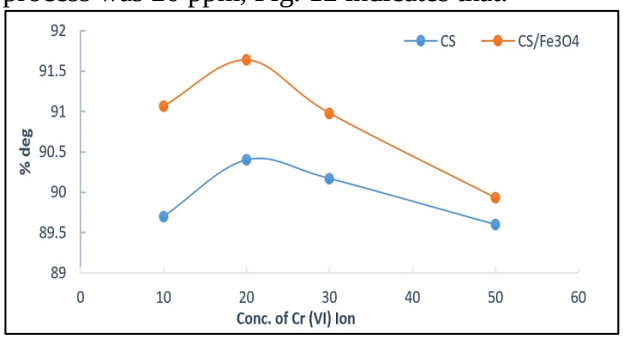

Figure 12. effect of varying Cr^{6+} ion concentration for M.B. 7 ppm concentration, $5*10^{-3}$ (H_2O_2 conc.) after 60 min, at 298K, pH= 7 on CS, CS/ Fe_3O_4 compound catalyst.

Effect of Temperature

An impact of temperature on M.B dye degradation has been researched by 7 ppm M.B., H_2O_2 concentration $5*10^{-3}$ M, 20ppm of Cr^{6+} ion pH= 7, Temp. 293, 303, 313 and 323 K & used CS/ Fe_3O_4 composite. After that, samples were withdrawn every 5 minutes. After UV irradiation. The determination of % deg. as shown in the following figures.

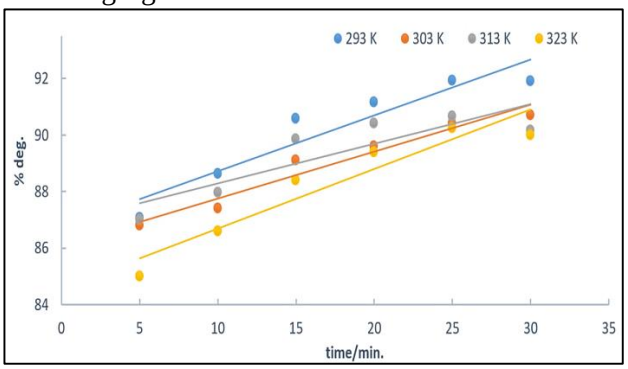

Figure 13. percentage degradation Variation of 7 ppm M.B with $5*10^{-3}$ H_2O_2 concentration, 20ppm of Cr^{6+}, by CS/ Fe_3O_4 composite with different temperature.

Kinetic Degradation Study

Using a CS/ Fe_3O_4 composite and 7 ppm M.B and $5*10^{-3}$ M of H_2O_2, the concentration of M.B. was followed with time according to different orders of reaction, the first-order equation was applied as shown in Fig. 14, according to equ. 2 [15]

$$\ln C_t = \ln C_0 - kt \qquad 2$$

Where: C_0: initial concentration of methylene blue. k: rate constant. t: time.

C_t: concentration of M.B after exposing to UV at specific.

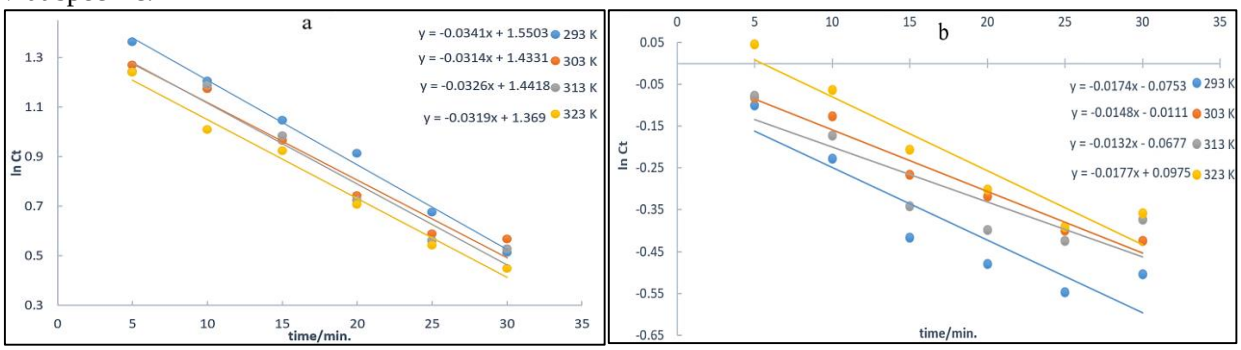

Figure 14. relation between Ln C_t and time for 7 ppm of methylene blue by a) CS, b) CS/ Fe_3O_4 composite at different temperatures

Fig. 15 illustrates how the Arrhenius equation was used to derive the kinetic parameter A, Ea: (Eqs 3&4) [16].

$k = A \exp(-Ea/RT)$ 3

$\ln k = \ln A - Ea/RT$ 4

Where T: is the absolute temperature (measured in kelvins), k (m^{-1}) is the rate constant, Ea is the reaction's activation energy (measured in kilojoules per mole), (A) is the pre-exponential factor, and R is a universal gas constant. In the rate equation, Ea stands for the activation of degradation (also known as the least amount of energy needed to initiate a chemical process). A stands for the pre-exponential component. The values of Ea and A are then determined by the slope and intercept of the Ln k against 1/T plot, respectively, the results, which are shown table 1.

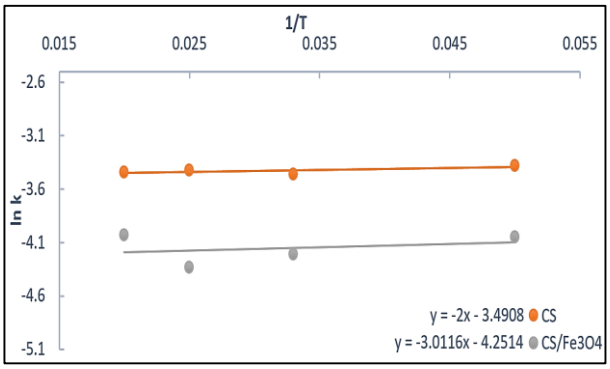

Figure 15. Arrhenius plots, relation Ln k with 1/T for 7 ppm M.B % deg. CS coating, CS/ Fe_3O_4 composite.

Table 1. Kinetic parameters for the materials CS and CS/ Fe_3O_4 composite.

metal	T(K)	k/(min.)*10^{-3}	Ln k	- Ea(J/mol)	A(min^{-1})
	293	0.0341	-3.378		
CS	303	0.0314	-3.461	16.628	0.031
	313	0.0326	-3.423		
	323	0.0319	-3.445		
	293	0.0174	-4.05		
CS/ Fe_3O_4	303	0.0148	-4.21	25.038	0.014
	313	0.0132	-4.33		
	323	0.0177	-4.03		

The degradation percentage (deg. %) with using CS/ Fe_3O_4 decreased with increasing temperature from 293-323 K and the value of Ea changed from 16.628 to 25.038 J/mol and (A) values (which related the number of sites) decreased from 0.031 to 0.014. This result shows the Anti- Arrhenius behavior, which may be related to formation of on complex between M.B. and empty d-orbital for (Cr^{6+}).

Test of Chemical Oxygen Demand (COD)

For detecting pollutants in wastewater and natural rivers, one widely used metric approach is COD [17]. After 60 minutes of irradiation, CS/ Fe_3O_4 composite reduced the carbon content to 83.6%, and the resulting solution was digested by potassium dichromate for 2 hours. The solution had a concentration of 7 ppm of MB at pH= 7, and the temperature was 298 K and 5*10^{-3} M H_2O_2 as detailed in Table 2.

Table 2. Chemical Oxygen Demand (COD) values of 7 ppm M.B on CS/Fe_3O_4 composites at H_2O_2 $5*10^{-3}$ M, pH= 7, and 298K.

Time/ min of digester	Initial COD mg/l	Final COD mg/l	Photo degradation Efficiency %
120	37.3	6.1	83.65

Conclusion:

In conclusion, methylene blue dye has the ability to degrade chitosan/Fe_3O_4 composite as catalyst in the presence of hexavalent chromium ion. AFM was successful in characterizing composites by measuring their average diameter and shape. After adding Cr to the CS/ Fe_3O_4 composite, the AFM image showed that the particle size increased and the efficiency of (M.B.) degradation increased. CS /Fe_3O_4 composite was used as a catalyst in the Photo-Fenton process, which was successful in removing the pollutants dye. The most effective irradiation period was determined to be 60 minutes. The results of the pH effect demonstrated that PH= 7 provided the best M.B dye degradation on CS/ Fe_3O_4 composite. The degradation of M.B dyes on the CS/ Fe_3O_4 composite was demonstrated to be temperature-dependent, increasing with in293 K temperature. The color was taken out, and the dye was changed into an organic. The degradation of M.B dyes on the CS/Fe_3O_4 composite was demonstrated to be temperature-dependent, increasing within 293 K temperature. The highest percentage of dye breaking down in the best studied conditions was 92%, This is an excellent percentage compared to the literature [18]. After the dye solution has been subjected to radiation for a longer amount of time, the color has been eliminated and the dye has been transformed into organic material (COD test after 2 hours is low or under range). According to the findings of the kinetic investigation, the M.B dye degradation on the CS/ Fe_3O_4 composite was well understood. Last but not least, it is advised to use the employed method (the photo Fenton process) to treat wastewater that contains organic compounds.

Acknowledgments

The authors would like to express their gratitude to the Department of Chemistry, College of Science, University of Baghdad.

Authors' Declaration:

- Conflicts of Interest: None.
- We hereby confirm that all the Figures and Tables in the manuscript are mine ours. Besides, the Figures and images, which are not mine ours, have been given the permission for re-publication attached with the manuscript.
- Ethical Clearance: The project was approved by the local ethical committee in University of Baghdad.

Authors' Contributions Statement:

Y. K. S. collected and analyzed the data and interpreted the results. K. A. S. Designed and planned the research plan, followed up the results, and proofread the manuscript.

References:

1. Su Dihan, J Liu, Y Zhong. Enhancing mechanical properties of silk fibroin hydrogel through restricting the growth of β-sheet domains. ACS Appl Mater Interfaces. 2017; 9(20): 17489-17498. https://doi.org/10.1021/acsami.7b04623
2. Mohammed Eman A, Souad A Mousa. Degradation of Dazomet by thermal Fenton and photo-Fenton processes under UV and sun lights at different temperatures. Baghdad Sci J. 2018; 15.2: 158-168. https://doi.org/10.21123/bsj.2018.15.2.0158
3. Sharma Abha, Ahmad Javed A, Flora S J S. Application of advanced oxidation processes and toxicity assessment of transformation products. Environ Res. 2018; 167: 223-233. https://doi.org/10.1016/j.envres.2018.07.010
4. Rueda Márquez, Juan José, Manuel M. Toxicity reduction of industrial and municipal wastewater by advanced oxidation processes (Photo-Fenton, UVC/H_2O_2, Electro-Fenton and Galvanic Fenton): a review. Catalysts. 2020; 10(6): 612. https://doi.org/10.3390/catal10060612
5. Al-Saade Khulood Abid Saleh; Al-Saidi Shatha Fadel; Juad Hamdia Hateem. Degradation of brilliant green by using a bentonite clay-based fe nanocomposite film as a heterogeneous photo-fenton catalyst. Baghdad Sci J. 2016; 13(3): 524-530. http://dx.doi.org/10.21123/bsj.2016.13.3.0524
6. Bibi Sidra, Awais A, Mohsin A. Photocatalytic degradation of malachite green and methylene blue over reduced graphene oxide (rGO) based metal oxides (rGO-Fe_3O_4/TiO_2) Nanocomposite under UV-visible light irradiation. J Environ Chem Eng. 2021; 9(4): 105580. https://doi.org/10.1016/j.jece.2021.105580
7. Cazetta A L, Vargas A M, Nogami E M, Kunita M H, Guilherme M R, Martins A C, et al. NaOH-activated carbon of high surface area produced from coconut shell: Kinetics and equilibrium studies from the methylene blue adsorption. J Chem Eng. 2011; 174(1): 117-125. https://doi.org/10.1016/j.cej.2011.08.058
8. Freire T M, Dutra L, Queiroz D, Ricardo S, Barreto K, Denardin J C, et al. Fast ultrasound assisted synthesis of chitosan-based magnetite nanocomposites as a modified electrode sensor. Carbohyd Polym. 2016; 151: 760-769. https://doi.org/10.1016/j.carbpol.2016.05.095

9. Muhi-Alden Yasser Yousef, Khulood A Saleh. Removing of Methylene Blue Dye from its Aqueous Solutions Using Polyacrylonitrile/Iron Oxide/Graphene Oxide. Iraqi J Sci. 2022; 2320-2330. https://doi.org/10.24996/ijs.2022.63.6.1
10. Kadhim Hakim H, Khulood A Saleh. Removing of copper ions from industrial wastewater using graphene oxide/chitosan nanocomposite. Iraqi J Sci. 2022; 1894-1908. https://doi.org/10.24996/ijs.2022.63.5.4
11. Sahib Saddam, Zaman W, F Ullah. Organometallic assembling of Chitosan-Iron oxide nanoparticles with their antifungal evaluation against Rhizopus oryzae. Appl Organomet Chem. 2019; 33(11): e5190. https://doi.org/10.1002/aoc.5190
12. Kadhim Hakim H, Khulood A Saleh. Removing cobalt ions from industrial wastewater using chitosan. Iraqi J Sci. 2022; 3251-3263. https://doi.org/10.24996/ijs.2022.63.8.1
13. Akbari Abbas, Sadani M. Managing sulfate ions produced by sulfate radical-advanced oxidation process using sulfate-reducing bacteria for the subsequent biological treatment. J Environ Chem Eng. 2018; 6(5): 5929-5937. https://doi.org/10.1016/j.jece.2018.09.004
14. Heidari Maryam, Sadeghi M. Degradation of diazinon from aqueous solutions by electro-Fenton process: effect of operating parameters, intermediate identification, degradation pathway, and optimization using response surface methodology (RSM). Sep Sci Technol. 2021; 56(13): 2287-2299. https://doi.org/10.1080/01496395.2020.1821060
15. Vinu R, Giridhar Madras. Kinetics of sonophotocatalytic degradation of anionic dyes with nano-TiO_2. Environ Sci Technol. 2009; 43(2): 473-479. https://doi.org/10.1021/es8025648
16. Arrhenius Svante. Über die Dissociationswärme und den Einfluss der Temperature auf den Dissociations grad der Elektrolyte. ZPC. 1889; 4(1): 96-116. https://doi.org/10.1515/zpch-1889-0408
17. Behin Jamshid, Mahmoudi M. Sodium hypochlorite as an alternative to hydrogen peroxide in Fenton process for industrial scale. Water Res. 2017; 121: 120-128. https://doi.org/10.1016/j.watres.2017.05.015
18. Zhang Kai,W Yang, K Zhang. Laccase immobilized on chitosan-coated Fe_3O_4 nanoparticles as reusable biocatalyst for degradation of chlorophenol. J Mol Struct. 2020; 1220: 128769. https://doi.org/10.1016/j.molstruc.2020.128769

تأثير الكروم السداسي على أكسدة صبغة المثيل الأزرق بواسطة متراكب الكيتوسان/ أوكسيد الحديد

خلود عبد صالح **يمان خالد صادق**

قسم الكيمياء، كلية العلوم، جامعة بغداد، بغداد، العراق.

الخلاصة:

لا تزال إزالة ايونات المعادن الثقيلة من أنظمة معالجة مياه الصرف الصناعي صعبة لأنها تحتوي على ملوثات عضوية. في هذه الدراسة، تم استخدام الهلاميات المائية المركبة الوظيفية مع نشاط تفاعل فنتون لتحلل الملوثات العضوية. تشكل جزيئات أوكسيد الحديد الثلاثي والكيتوسان والمواد الأخرى الهيدروجيل. العوامل المحتلفة التي أثرت على نشاط فنتون الضوئي. تشمل الأس الهيدروجيني وتركيز بيروكسيد الهيدروجين ودرجة الحرارة وفترة التعرض. تم استخدام مجهر القوة الذرية (AFM) لفحص مورفولوجيا المركب ومتوسط قطره. وجد انه بعد 60 دقيقة من التعرض للأشعة الفوق البنفسجية، تسبب المتراكب المحضر في تدهور صبغة المثيل الأزرق بنسبة 92% في غضون ذلك، بعد ساعة واحدة من الإشعاع، انخفضت نسبة الطلب على الأوكسجين (COD) لتحطيم المحتوى الكاربوني إلى 6.1 ملغم/لتر .

الكلمات المفتاحية: الامتزاز ، متراكب،CS/Fe_3O_4 الانحلال، صبغة المثيل الأزرق، تفاعل فوتو-فنتون.